JHEP

Published for SISSA by Springer

Received: June 21, 2022
Accepted: August 25, 2022
Published: September 14, 2022

Instability of the electroweak vacuum in Starobinsky inflation

Qiang Li,[a] **Takeo Moroi,**[a] **Kazunori Nakayama**[b,c] **and Wen Yin**[b]

[a] *Department of Physics, The University of Tokyo, Tokyo 113-0033, Japan*

[b] *Department of Physics, Tohoku University, Sendai 980-8578, Japan*

[c] *International Center for Quantum-field Measurement Systems for Studies of the Universe and Particles (QUP), KEK, 1-1 Oho, Tsukuba, Ibaraki 305-0801, Japan*

E-mail: qiangli@hep-th.phys.s.u-tokyo.ac.jp, moroi@phys.s.u-tokyo.ac.jp, kazunori.nakayama.d3@tohoku.ac.jp, yin.wen.b3@tohoku.ac.jp

Abstract: We study the stability of the electroweak vacuum during and after the Starobinsky inflation, assuming the existence of the non-minimal Higgs coupling to the Ricci scalar. In the Starobinsky inflation, there exists R^2 term (with R being the Ricci scalar), which modifies the evolution equation of the Higgs field. We consider the case that the non-minimal coupling is sizable so that the quantum fluctuation of the Higgs field is suppressed and that the Higgs amplitude is settled near the origin during the inflation. In such a case, the Higgs amplitude may be amplified in the preheating epoch after inflation because of the parametric resonance due to the non-minimal coupling. We perform a detailed analysis of the evolution of the Higgs field in the preheating epoch by a numerical lattice simulation and derive an upper bound on the non-minimal coupling constant ξ in order to realize the electroweak vacuum in the present universe. We find that the upper bound on ξ in the Starobinsky inflation model is more stringent than that in conventional inflation models without the R^2 term.

Keywords: Cosmology of Theories BSM, Early Universe Particle Physics, Higgs Properties

ArXiv ePrint: 2206.05926

https://doi.org/10.1007/JHEP09(2022)102

JHEP09(2022)102

Contents

JHEP09(2022)102

1 Introduction

Stability of the electroweak vacuum, in which we are living, is highly non-trivial in quantum field theory. Even if the electroweak vacuum, at which the Higgs vacuum expectation value (VEV) is given by $\langle h \rangle \simeq 246$ GeV, corresponds to a local minimum of the Higgs potential, there may exist another minimum of the potential at which the energy density becomes smaller than that of the electroweak vacuum. If so, the electroweak vacuum becomes metastable and it decays into the true vacuum via the quantum tunneling effect [1–8]. The metastability of the electroweak vacuum occurs in the standard model as well as in certain models with physics beyond the standard model.

In the standard model, it is well known that the Higgs quartic coupling, which is positive at the electroweak scale, may become negative at higher energy scale due to the renormalization group effect. Using the central values of standard-model parameters, the Higgs quartic coupling constant becomes negative at the instability scale of $\sim O(10^{10})$ GeV. The negativity of the quartic coupling constant indicates that the electroweak vacuum is not the absolute minimum of the potential and that it is metastable. We emphasize that the metastability of the electroweak vacuum does not imply the difficulty to realize the electroweak vacuum in the present universe. Indeed, in the standard model, the lifetime of the electroweak vacuum is much longer than the present cosmic time [9–17]. Thus, once the Higgs field settles to the electroweak vacuum in the early universe, we can safely live in the electroweak vacuum even if the standard model is valid up to a very high energy scale.

The behavior of the Higgs field is, however, highly non-trivial in the early universe. In particular, during and after the inflation, the Higgs field is influenced by the dynamics

of the rapid expansion of the universe as well as by the motion of the inflaton. During the inflation, the quantum fluctuation of the Higgs field may make the Higgs amplitude larger than the instability scale; in such a case, the Higgs shows a run-away behavior during inflation due to the negative quartic coupling, which provides a cosmic history inconsistent with the present universe [18–28]. Such a problem can be avoided if the Higgs field has a non-minimal coupling to the Ricci scalar. The non-minimal coupling induces an effective mass term of the Higgs during the inflation which stabilizes the Higgs potential if the sign of the non-minimal coupling constant is properly chosen. Hereafter, we concentrate on the case with the non-minimal coupling of the Higgs. Even though the non-minimal coupling stabilizes the Higgs potential during the inflation, it may cause an instability after the inflation [29–38]. With the non-minimal coupling, the effective mass of the Higgs may have significant time-dependence because of the oscillatory behavior of the Ricci scalar after inflation. Then, the Higgs amplitude may be amplified due to the parametric resonance [39–43] or tachyonic resonance [44–46] at the preheating epoch after the inflation; if the effect of the parametric resonance is too large, the Higgs amplitude exceeds the instability scale and the Higgs shows the run-away behavior. The effect of the parametric resonance is more enhanced with larger value of the non-minimal coupling, and we obtain an upper bound on the non-minimal coupling to realize the electroweak vacuum in the present universe.

The dynamics of the Higgs field after inflation depends on couplings of the Higgs to the inflaton and Ricci scalar as well as on the model of the inflation. The upper bound on the non-minimal coupling has been studied in simple inflation model in which the gravity sector is described by the Einstein-Hilbert action [29–38]. Based on the recent observations of cosmic density perturbations, however, an inflation model with R^2 term (with R being the Ricci scalar), which is called the Starobinsky inflation [47], has been attracting many attentions. The Starobinsky inflation predicts the scalar spectral index and the tensor-to-scalar ratio consistent with the observations [48]. In addition, the Starobinsky inflation provides an interesting possibility of producing hidden-sector dark matter via the decay of the inflaton [49–52]. Phenomenology based on the Starobinsky inflation crucially depends on the stability of the electroweak vacuum during and after the inflation. Importantly, the evolution equation of the Higgs field in Starobinsky inflation differs from that in simple inflation models (without the R^2 term). Thus, the dedicated study about the stability of the electroweak vacuum is necessary for the case of the Starobinsky inflation.

In this paper, we consider the stability of the electroweak vacuum during and after the Starobinsky inflation. In particular, we study in detail the Higgs dynamics after inflation by a numerical lattice simulation. Then, we derive an upper bound on the non-minimal coupling constant to realize the electroweak vacuum in the present universe.

The organization of this paper is as follows. In section 2, we give an overview of the Starobinsky inflation model as well as the behavior of the Higgs and inflaton potential in the framework of our interest. In section 3, we discuss the stability of the electroweak vacuum during and after the Starobinsky inflation. In section 4, we perform a lattice simulation to study the stability of the electroweak vacuum in the preheating epoch after inflation and derive an upper bound on the non-minimal coupling constant. Section 5 is devoted to conclusions and discussion.

JHEP09(2022)102

2 Model

In this section, we summarize the basic features of the Starobinsky inflation model with the Higgs non-minimal coupling to gravity. We also give a brief summary of the properties of the Higgs potential in the standard model.

2.1 Lagrangian

We start with introducing the total Lagrangian of the model we consider. In the Jordan frame, the action has the following form:

$$S = S_{\rm inf} + S_{\rm Higgs} + S_{\rm int}, \tag{2.1}$$

where $S_{\rm inf}$, $S_{\rm Higgs}$, $S_{\rm int}$ are actions of the inflation sector, the Higgs sector and the interaction between Higgs and gravity, respectively. Taking the unitary gauge $\Phi = (0, h/\sqrt{2})^T$ (with Φ being the Higgs doublet while h being a real scalar field), they are given by [47]

$$S_{\rm inf} = \int d^4x\sqrt{-\hat{g}}\left[-\frac{M_{\rm Pl}^2}{2}\left(\hat{R} - \frac{1}{6\mu^2}\hat{R}^2\right)\right], \tag{2.2}$$

$$S_{\rm Higgs} = \int d^4x\sqrt{-\hat{g}}\left(\frac{1}{2}\hat{g}^{\mu\nu}\partial_\mu h\partial_\nu h - \frac{\lambda}{4}h^4\right), \tag{2.3}$$

$$S_{\rm int} = \int d^4x\sqrt{-\hat{g}}\ \frac{1}{2}\xi\hat{R}h^2, \tag{2.4}$$

where fields with hat are defined in the Jordan frame, $M_{\rm Pl} \simeq 2.4 \times 10^{18}$ GeV is the reduced Planck scale, and ξ is the Higgs-gravity non-minimal coupling constant.[1] Hereafter, we consider the case of ξ being non-negative.[2] The Higgs quartic coupling constant λ depends on the renormalization scale Q. More detail about the scale dependence of λ will be discussed in the next subsection.

By introducing an auxiliary field φ [53], the action (2.1) can be rewritten as

$$S = \int d^4x\sqrt{-\hat{g}}\left[-\frac{M_{\rm Pl}^2}{2}\left(1 - \frac{\varphi}{3\mu^2} - \frac{\xi}{M_{\rm Pl}^2}h^2\right)\hat{R} - \frac{M_{\rm Pl}^2\varphi^2}{12\mu^2} + \frac{1}{2}\hat{g}^{\mu\nu}\partial_\mu h\partial_\nu h - \frac{\lambda}{4}h^4\right]. \tag{2.5}$$

Note that the Euler-Lagrange equation of φ gives

$$\varphi = \hat{R}, \tag{2.6}$$

and by substituting back to (2.5) we obtain the original action.

For the study of the stability of the electroweak vacuum, it is convenient to work in the Einstein frame. With the conformal transformation of the metric

$$g_{\mu\nu} = \Omega^2\hat{g}_{\mu\nu}, \tag{2.7}$$

[1] We neglect the bare Higgs quadratic term which is irrelevant for our discussion.

[2] In our convention, the conformal coupling is $\xi = 1/6$. If $\xi < 0$, the non-minimal coupling induces a tachyonic mass term of the Higgs field, so the electroweak vacuum is destabilized during inflation [24].

JHEP09(2022)102

where

$$\Omega^2 = 1 - \frac{\varphi}{3\mu^2} - \frac{\xi}{M_{\rm Pl}^2}h^2, \tag{2.8}$$

we can eliminate the non-minimal couplings and obtain the action in the Einstein frame as

$$S = \int d^4x\sqrt{-g}\left[-\frac{M_{\rm Pl}^2}{2}R + \frac{1}{2}g^{\mu\nu}\partial_\mu\phi\partial_\nu\phi + \frac{1}{2}e^{-\chi}g^{\mu\nu}\partial_\mu h\partial_\nu h - V(\phi,h)\right], \tag{2.9}$$

where we have defined χ and the scalaron field ϕ through

$$\frac{\phi}{M_{\rm Pl}} = \sqrt{\frac{3}{2}}\ln\Omega^2, \quad \chi = \sqrt{\frac{2}{3}}\frac{\phi}{M_{\rm Pl}}. \tag{2.10}$$

Although ϕ (or, equivalently, φ) was introduced as the auxiliary field, it becomes a physical degree of freedom; with the R^2 term, there exists an extra physical degree of freedom in the metric other than the tensor modes, and it is converted to ϕ by the conformal transformation. In addition, the scalar potential $V(\phi, h)$ is given by

$$V(\phi,h) = \frac{3\mu^2M_{\rm Pl}^2}{4}\left(1 - e^{-\chi} + \frac{\xi}{M_{\rm Pl}^2}e^{-\chi}h^2\right)^2 + \frac{\lambda}{4}e^{-2\chi}h^4. \tag{2.11}$$

If the initial amplitude of ϕ is larger than $M_{\rm Pl}$, an approximate de Sitter space is realized and the inflation occurs. This can be understood by studying the potential of ϕ (with neglecting the Higgs field):

$$V \simeq \frac{3\mu^2M_{\rm Pl}^2}{4}\left[1 - \exp\left(-\sqrt{\frac{2}{3}}\frac{\phi}{M_{\rm Pl}}\right)\right]^2. \tag{2.12}$$

One can see that the potential becomes flat when $\phi \gg M_{\rm Pl}$. Due to the flatness of this potential at large ϕ, the slow-roll inflation (called Starobinsky inflation) can happen. The expansion rate during the inflation is evaluated as

$$H_{\rm inf} \simeq \frac{1}{2}\mu. \tag{2.13}$$

We define t_* as the time when the slow roll parameter, $\epsilon \equiv -\dot{H}/H^2$, becomes equal to unity (i.e., end of the inflation); at the time of $t = t_*$,

$$\epsilon(t_*) = 1, \quad \phi_* \equiv \phi(t_*) \simeq 0.97M_{\rm Pl}, \quad \dot{\phi}_* \equiv \dot{\phi}(t_*) \simeq -3.75\times10^{-6}M_{\rm Pl}^2. \tag{2.14}$$

In the Starobinsky inflation model, the curvature perturbation amplitude A_s, the scalar spectral index n_s, and the tensor-to-scalar ratio r are evaluated as

$$A_s(k) \simeq \frac{1}{24\pi^2}\frac{\mu^2}{M_{\rm Pl}^2}N_e^2, \tag{2.15}$$

$$n_s(k) - 1 \simeq -\frac{2}{N_e}, \tag{2.16}$$

$$r(k) \simeq \frac{12}{N_e^2}, \tag{2.17}$$

JHEP09(2022)102

where N_e is the e-folding number at which the mode with comoving wavenumber k exits the horizon and is related to the scalaron amplitude as

$$N_e \simeq \frac{3}{4} \exp\left(\sqrt{\frac{2}{3}} \frac{\phi}{M_{\rm Pl}}\right). \tag{2.18}$$

Taking $N_e(k = 0.05{\rm Mpc}^{-1}) \simeq 56$, the observed value of $A_s \simeq 2.1 \times 10^{-9}$ [54] gives

$$\mu \simeq 3.1 \times 10^{13}\ {\rm GeV}, \tag{2.19}$$

which will be used for our numerical analysis, while the scalar spectral index and the tensor-to-scalar ratio are well within the allowed region [48, 55].

We also note here that, during the inflation, the Higgs field acquires an effective mass squared of $\sim 12\xi H_{\rm inf}^2$. Thus, if ξ is larger than ~ 0.1, the Higgs field is forced to be at the origin during the inflation.

2.2 Higgs potential at quantum level

Next, we discuss the behavior of the Higgs potential with including the quantum effects. The Higgs potential is dominated by the quartic term as indicated in the previous section. The coupling constant λ for the quartic interaction of the Higgs has scale dependence and, as is well known, it may become negative at the scale much higher than the electroweak scale. In order to take account of the scale dependence of the quartic coupling constant, we evaluate λ at the scale of the Higgs amplitude. Because we will deal with the case that the Higgs field is inhomogeneous, we approximate the Higgs potential as

$$V_{\rm Higgs} = \frac{1}{4}\lambda\left(Q = \sqrt{\langle h^2 \rangle}\right) h^4, \tag{2.20}$$

where $\lambda(Q)$ denotes the quartic coupling constant at the renormalization scale Q and $\langle \cdots \rangle$ is the spatial average. The bare mass term of the Higgs is neglected because it is irrelevant for our following discussion.

In our analysis, we assume the particle content of the standard model (as well as inflaton) and study the scale dependence of λ. The renormalization group behavior of λ is sensitive to standard model parameters, in particular, the top quark mass M_t, the strong coupling constant α_s, and the Higgs mass.

Let us first consider the top quark pole mass M_t. It can be obtained from the kinematics in the top anti-top events. The latest PDG average gives [56]

$$M_t = 172.76 \pm 0.3\,{\rm GeV}. \tag{2.21}$$

We take the central value of M_t as our canonical value and, in order to take account of the top-mass uncertainty, we also provide the numerical results with several values of the top mass. For the strong coupling constant, we adopt [56]

$$\alpha_s(m_Z) = 0.1179(9). \tag{2.22}$$

JHEP09(2022)102

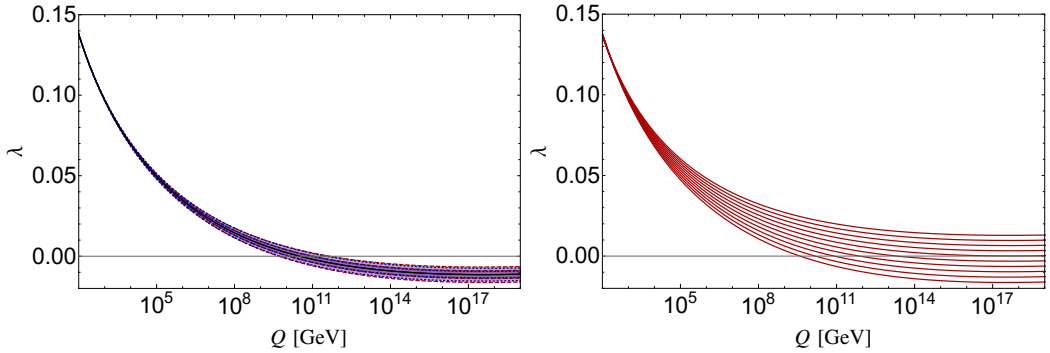

Figure 1. The Higgs quartic coupling λ as a function of the renormalization scale $\mu_{\rm RG}$ with different input standard-model couplings. In the left panel we show the running λ with the central values of the measured standard-model couplings including (2.21) (black solid line). The blue dotted (red dashed) lines indicate the 1 and 2 σ range by varying M_t (α_s) according to eq. (2.22) (eq. (2.21)). In the right panel, we show the scale dependence of λ with $M_t = 169.0, 169.5, 170.0, \cdots, 173.5\,\text{GeV}$ from top to bottom.

In addition, the Higgs boson mass is given by [56]

$$m_h = 125.25 \pm 0.17 \text{ GeV}. \tag{2.23}$$

We show the scale dependence of λ in figure 1. We use the `SMDR` code [57], which partially includes 3, 4, and 5 loop effects, to numerically solve the renormalization group equations in the standard model. In the left panel, M_t and α_s are varied within 2 σ ranges around their central values. We can see that even adopting such uncertainties in the standard model parameters, λ becomes negative at a high scale and the Higgs potential is metastable. Using the central values of the standard model parameters, we find the instability scale, define as $\lambda(\Lambda_I) = 0$, to be

$$\Lambda_I \simeq 3.3 \times 10^{10}\,\text{GeV}. \tag{2.24}$$

The instability scale may vary by an order of magnitude when we take account of the $\sim 2\sigma$ uncertainties. In the right panel, we show the scale dependence for several values of M_t while taking central values of other parameters. The Higgs potential becomes absolutely stable for $M_t \lesssim 171\text{GeV}$, which is inconsistent with eq. (2.21) at $\sim 6\sigma$ level. Thus in the standard model, the Higgs potential is very likely to have a radiative instability.

2.3 Effective mass of the Higgs

The Higgs dynamics becomes highly non-trivial due to the presence of inflaton field. In the flat space-time (i.e., when the inflaton is at the minimum of its potential), the Higgs field can just stay at the electroweak vacuum. During and after the inflation, on the contrary, the inflaton is in motion which affects the dynamics of the Higgs field.

Although our numerical lattice simulation is performed based on the action given in eq. (2.9), it is also instructive to consider the frame in which the Higgs field is canonically normalized. Such a frame can be realized with the following transformation:

$$h_c \equiv e^{-\chi/2} h. \tag{2.25}$$

JHEP09(2022)102

Then, the total action is found to be

$$S = \int d^4x\sqrt{-g}\left[-\frac{M_{\rm Pl}^2}{2}R + \frac{1}{2}g^{\mu\nu}\partial_\mu\phi\partial_\nu\phi + \frac{1}{2}g^{\mu\nu}\partial_\mu h_c\partial_\nu h_c - \tilde{V}(\phi, h_c)\right], \tag{2.26}$$

where[3]

$$\tilde{V}(\phi, h_c) = \frac{3\mu^2 M_{\rm Pl}^2}{4}(1 - e^{-\chi})^2 + \frac{1}{2}m_{\rm eff}^2 h_c^2 + \frac{1}{4}\left(\lambda + \frac{3\mu^2}{M_{\rm Pl}^2}\xi^2\right)h_c^4, \tag{2.27}$$

with

$$m_{\rm eff}^2 \equiv \frac{1}{2\sqrt{-g}}\partial_\mu\left(\sqrt{-g}g^{\mu\nu}\partial_\nu\chi\right) - \frac{1}{4}g^{\mu\nu}(\partial_\mu\chi)(\partial_\nu\chi) + 3\mu^2(1 - e^{-\chi})\xi. \tag{2.28}$$

Because the inflaton field is (almost) homogeneous, $m_{\rm eff}^2$ can be expressed as

$$m_{\rm eff}^2 \simeq \frac{1}{\sqrt{6}M_{\rm Pl}}(\ddot{\phi} + 3H\dot{\phi}) - \frac{1}{6M_{\rm Pl}^2}\dot{\phi}^2 + 3\mu^2\left[1 - \exp\left(-\sqrt{\frac{2}{3}}\frac{\phi}{M_{\rm Pl}}\right)\right]\xi, \tag{2.29}$$

where H is the expansion rate of the universe. Using the relation $R \simeq (\dot{\phi}^2 - 4V)/M_{\rm Pl}^2$, $m_{\rm eff}^2$ can be also expressed as

$$m_{\rm eff}^2 \simeq -\xi R + \left(\xi - \frac{1}{6}\right)\left(\frac{\dot{\phi}^2}{M_{\rm Pl}^2} + \sqrt{6}\frac{\partial_\phi V}{M_{\rm Pl}}\right). \tag{2.30}$$

We can see that the effective Higgs mass squared is dependent on the inflaton amplitude. During the inflation, the inflaton is slowly rolling with its amplitude much larger than $M_{\rm Pl}$ and hence, if ξ is sizable, $m_{\rm eff}^2 \simeq 3\xi\mu^2 \simeq 12\xi H_{\rm inf}^2$ during the inflation. In particular, if $\xi \gtrsim O(0.1)$, $m_{\rm eff}$ becomes of the order of the expansion rate and the quantum fluctuation during the inflation is suppressed. On the contrary, in the preheating epoch, ϕ is oscillating and hence $m_{\rm eff}^2$ becomes highly time-dependent. It is also clearly seen in eq. (2.30) that there appear additional terms proportional to $(\xi - 1/6)$ which is characteristic for the Starobinsky inflation model. Thus we cannot simply apply the bound on ξ obtained for inflation models with Einstein gravity in the case of Starobinsky inflation. In the following sections, we will see details of the Higgs dynamics with fully taking account of these effects.

3 Instability of the electroweak vacuum

Now, we are in the position to discuss the stability of the electroweak vacuum in the Starobinsky inflation model. In this section, we give an overview of the Higgs dynamics. A detailed study of the Higgs dynamics based on a lattice simulation will be given in the next section. In the Starobinsky inflation model, the vacuum instability may be a serious issue in two epochs: inflationary epoch and preheating epoch. The Higgs dynamics in these epochs are considered in the following, taking into account important features in the Starobinsky model.

[3]As shown in eq. (2.27), the Higgs quartic coupling we observe should be $\lambda + \frac{3\mu^2}{M_{\rm Pl}^2}\xi^2$. With the model parameters of our interest, i.e., $\mu \simeq 3.1 \times 10^{13}$ GeV and $\xi \lesssim O(1)$, the second term is numerically irrelevant and we neglect its effects.

JHEP09(2022)102

3.1 Higgs instability in the early Universe: $|\xi| \ll 1$

During the inflationary epoch, the Higgs field acquires quantum fluctuation. In particular, if the effective mass of the Higgs during inflation is much smaller than the expansion rate $H_{\rm inf}$, the amplitude of the quantum fluctuation is typically $H_{\rm inf}$. In the case of the Starobinsky inflation, such a quantum fluctuation is dangerous because $H_{\rm inf} \simeq 1.6 \times 10^{13}\,{\rm GeV}$ is much larger than the instability scale Λ_I. In particular, when $|\xi| \ll 1$, for which the effective Higgs mass during the inflation is negligible, the Higgs amplitude becomes as large as $H_{\rm inf}$ within $O(10)$ e-folds even if the initial amplitude vanishes [18–28].[4]

If the Higgs amplitude h becomes larger than $\sim \Lambda_I$ during inflation due to the quantum fluctuation, h may have run-away behavior because of the negative quartic coupling for $h \gtrsim \Lambda_I$, resulting in a failure to realize the electroweak vacuum after inflation. The detailed evolution of the Higgs amplitude is model dependent; in the case of our interest, the evolution of the Higgs amplitude should be studied including the effects of Higgs-inflaton coupling. In particular, in the case of the Starobinsky inflation, the effective mass of the Higgs is induced, as shown in the previous section, which may affect the dynamics of the Higgs field.

In order to see how the Higgs field evolves if the initial amplitude is as large as $\sim H_{\rm inf}$, we solve the classical equation of motion. Here, we neglect the spatial dependence of the Higgs field because the non-vanishing Higgs amplitude due to the quantum fluctuation is particularly important for the over-horizon mode. In addition, we consider the case that the energy density of the Higgs is sub-dominant. Then, in the frame in which the Higgs field is canonically normalized, the evolution equation is given by

$$\ddot{h}_c + 3H\dot{h}_c + m_{\rm eff}^2 h_c + \lambda(Q = h_c)h_c^3 = 0, \tag{3.1}$$

where, in the present calculation, the expansion rate is evaluated as

$$H = \sqrt{\frac{1}{3M_{\rm Pl}^2}\left[\frac{1}{2}\dot{\phi}^2 + \frac{1}{2}\dot{h}_c^2 + \tilde{V}(\phi, h_c)\right]}. \tag{3.2}$$

We numerically solve the above differential equation and the equation of motion (EoM) of the inflaton simultaneously. The initial condition is imposed at the end of the inflation (see eq. (2.14)).

We first consider the case of $|\xi| \ll 0.1$, for which the effective mass during the inflation is negligible (see the discussion in the previous section). Then, the Higgs amplitude at the end of inflation is expected to be $\sim H_{\rm inf}$ or larger. We numerically solve eq. (3.1) with such an initial condition to see if the electroweak vacuum can be realized in the present epoch.

In figure 2, we show the evolution of the Higgs amplitude as a function of time, taking several different values of $h(t_*)$ and $\xi = 0$. We can see that the Higgs amplitude shows the run-away behavior when $h(t_*) \gtrsim 0.1 H_{\rm inf}$. Our results indicate that, in the Starobinsky inflation model, the electroweak vacuum at the present universe cannot be realized if $|\xi| \ll 1$.

[4] If the Higgs amplitude is much larger than $H_{\rm inf}/\sqrt{|\lambda|}$ at the horizon exit, the Higgs field may roll to the true vacuum during the inflation. The inflation is then terminated due to the negatively large vacuum energy of Higgs potential. We do not consider such a case.

JHEP09(2022)102

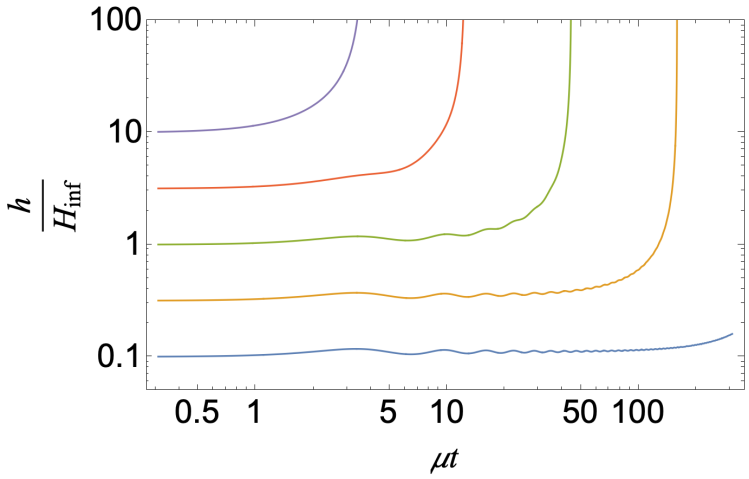

Figure 2. Evolution of the Higgs amplitude after inflation, taking $h(t_*) = 0.1H_{\rm inf}$ (blue), $0.3H_{\rm inf}$ (orange), $H_{\rm inf}$ (green), $3H_{\rm inf}$ (red), and $10H_{\rm inf}$ (purple), from the bottom to the top. The non-minimal coupling is taken to be $\xi = 0$.

The instability due to the quantum fluctuation during the inflation can be avoided if the non-minimal coupling of the Higgs to gravity is sizable. As discussed in the previous section, if $\xi \gtrsim O(0.1)$, the effective mass of the Higgs during the inflation is as large as $\sim H_{\rm inf}$, with which the $h(t_*)$ can be much smaller than $H_{\rm inf}$. It is known that the quantum fluctuation during the inflation is suppressed exponentially if $\xi > \frac{3}{16}$ [24]; in the following discussion, we consider such a case.

3.2 Higgs instability during the preheating

The quantum fluctuation of the Higgs field during the inflation can be suppressed if $\xi \gtrsim O(0.1)$. In such a case, however, the Higgs amplitude may be amplified due to the parametric or tachyonic resonance at the preheating after the inflation [29, 30].

Importance of the parametric resonance can be understood by studying the behavior of the Higgs effective mass in the preheating epoch. After the inflation, the inflaton starts to oscillate around the minimum of the potential with the amplitude smaller than the Planck scale. Then the effective mass of the Higgs (2.29) in the preheating epoch is approximately given by

$$m_{\rm eff}^2\Big|_{\rm preheating} \simeq (6\xi - 1)\frac{\mu^2\phi}{\sqrt{6}M_{\rm Pl}} + (1 - 2\xi)\frac{\mu^2\phi^2}{2M_{\rm Pl}^2} - \frac{\dot{\phi}^2}{6M_{\rm Pl}^2}. \tag{3.3}$$

The first term is dominant for $|\phi| \ll M_{\rm Pl}$ and we focus on it for the moment.[5] With this oscillating effective mass, the evolution of the Higgs amplitude is well described by the Mathieu equation.[6] For the time scale much shorter than H^{-1}, for which we can neglect

[5] Note, however, that it is the second and third terms that give non-vanishing contributions to the effective mass squared after time average. By using $\langle\dot{\phi}^2\rangle \simeq \mu^2\langle\phi^2\rangle$, we find $\langle m_{\rm eff}^2|_{\rm preheating}\rangle \simeq (1 - 3\xi)H^2$. Thus it gives tachyonic mass for $\xi > 1/3$.

[6] In the limit of small inflaton oscillation amplitude, the first term of (3.3) describes the perturbative decay of the inflaton into the Higgs boson pair (c.g. refs. [58, 59]).

JHEP09(2022)102

the effect of the cosmic expansion and approximate the motion of the inflaton as

$$\phi|_{\rm preheating} \sim \bar{\phi} \cos \mu t, \tag{3.4}$$

the Fourier amplitude of the Higgs, denoted as h_k with k being the wave number, is governed by

$$\left(\frac{d^2}{dz^2} + A_k + 2q \cos 2z \right) h_k = 0, \tag{3.5}$$

where $z = \mu t/2$, $A_k = 4k^2/\mu^2$ and

$$q \equiv \sqrt{\frac{2}{3}} \frac{\bar{\phi}}{M_{\rm Pl}} (6\xi - 1). \tag{3.6}$$

Here, the effect of the quartic coupling, which is unimportant unless the Higgs amplitude becomes large, is neglected. At the onset of the preheating epoch, at which the inflaton amplitude is order of magnitude smaller than $\sim M_{\rm Pl}$, the broad resonance condition, $q \gtrsim 1$, is satisfied for $\xi \gtrsim O(1)$. When ξ is larger than a few, the Higgs Fourier amplitudes in the resonance modes become significantly populated. Such a tachyonic preheating process may make the Higgs amplitude larger than Λ_I and cause a run-away behavior of the Higgs field. Thus, we expect that the non-minimal coupling constant ξ is bounded from above to realize the electroweak vacuum in the present universe.

In deriving the upper bound on ξ, a careful analysis is necessary. Once the Higgs amplitude becomes sizable, the quartic interaction of the Higgs becomes important. In addition, as discussed in the previous section, the EoMs of the inflaton and Higgs are coupled so that the EoMs should be solved simultaneously to take account of the effects of the back reaction to the inflaton dynamics from the particle creation due to the parametric resonance. For the precise study of the dynamics of the inflaton and Higgs fields taking into account the above mentioned effects as well as the cosmic expansion, we perform a numerical lattice simulation in the next section.

4 Higgs dynamics after inflation

In this section, we study the dynamics of the Higgs field in the preheating epoch in detail. Even if the Higgs quantum fluctuation during the inflation is suppressed by, for example, the mass term from the Higgs non-minimal coupling, the Higgs field may be resonantly excited in the preheating epoch. Once the averaged amplitude of the Higgs field becomes larger than $\sim \Lambda_I$, Higgs may show the run-way behavior because of the negative quartic coupling [30, 32, 34]. As mentioned earlier, the effect of the parametric resonance is expected to be more important for larger value of ξ. Too large ξ should result in the instability of the electroweak vacuum. The upper bound on ξ is studied in detail in the following.

The resonant production is effective, particularly for the modes in the instability bands. Because the oscillation frequency of the inflaton is $\sim \mu$ in the preheating epoch, the wave number of the instability modes are $k \sim \frac{1}{2}\mu$, μ, $\frac{3}{2}\mu$, $\cdots$. For the study of the parametric

JHEP09(2022)102

resonance, the inclusion of the spatial dependence of the Higgs amplitude is crucial. We should also consider the effects of cosmic expansion. In order to take account of these, we use a numerical lattice simulation to study the dynamics of the Higgs field after the Starobinsky inflation.

We perform our lattice simulation based on the Einstein frame action given in eq. (2.9). The equation of motion of the inflaton is given by

$$\ddot{\phi} + 3H\dot{\phi} - \frac{1}{a^2}\partial_i^2\phi + \frac{1}{\sqrt{6}M_p}e^{-\chi}\left[\dot{h}^2 - \frac{1}{a^2}(\partial_i h)^2\right] + \frac{\partial V}{\partial \phi} = 0, \tag{4.1}$$

while that of the Higgs field is

$$\ddot{h} + 3H\dot{h} - \frac{1}{a^2}\partial_i^2 h - \sqrt{\frac{2}{3}}\frac{1}{M_p}\left[\dot{\phi}\dot{h} - \frac{1}{a^2}(\partial_i\phi)(\partial_i h)\right] + e^{\chi}\frac{\partial V}{\partial h} = 0. \tag{4.2}$$

We evaluate the expansion rate by using the spatially averaged energy density as

$$H = \sqrt{\frac{\langle\rho\rangle}{3M_{\rm Pl}^2}}, \tag{4.3}$$

where

$$\rho = \frac{1}{2}\left[\dot{\phi}^2 + \frac{1}{a^2}(\partial_i\phi)^2\right] + \frac{1}{2}e^{-\chi}\left[\dot{h}^2 + \frac{1}{a^2}(\partial_i h)^2\right] + V(\phi, h). \tag{4.4}$$

Compared to the conventional inflation models without the R^2 term, there are several differences in the equations of motion; in eq. (4.2), we can find cross terms of the inflaton and the Higgs in the square bracket and also a factor of e^{χ} in front of the derivative of the potential, which do not exist in the case of the conventional inflation. They may affect the dynamics of the Higgs field.

We are interested in the Higgs dynamics with the scalar potential given in eq. (2.11). The potential is, however, unbounded below with taking into account the scale dependence of the quartic coupling constant λ. Such a potential is problematic for our lattice simulation because it makes the numerical calculation unstable. We add a h^6 term to stabilize the potential to cure this difficulty. In our lattice simulation, we use the following potential:

$$V(\phi, h) = \frac{3\mu^2 M_{\rm Pl}^2}{4}\left(1 - e^{-\chi} + \frac{\xi}{M_{\rm Pl}^2}e^{-\chi}h^2\right)^2 + \frac{\lambda\left(Q = \sqrt{\langle h^2\rangle}\right)}{4}e^{-2\chi}h^4 + \frac{c}{6M_{\rm Pl}^2}e^{-2\chi}h^6, \tag{4.5}$$

where c is a positive constant. With our choice of c, the Higgs potential at $H \sim \Lambda_I$ is almost unaffected although the h^6 term changes the behavior of the potential at large Higgs amplitude. Thus, the onset of the instability is not affected by the h^6 term in our analysis, as we show in the following. The Higgs potential given in eq. (4.5) has its minimum $h = h_{\rm min}$ which is given by

$$h_{\rm min} \simeq \sqrt{\frac{|\lambda(Q = h_{\rm min})|}{c}}M_{\rm Pl}, \tag{4.6}$$

where $\lambda(Q = h_{\rm min}) < 0$ is assumed. We take $c = 2 \times 10^3$ unless otherwise mentioned.

JHEP09(2022)102

In the lattice simulation, the field amplitudes of the inflaton and the Higgs field at the lattice sites are followed by numerically solving eqs. (4.1) and (4.2). We modify the GABE code [60], which uses the second-order Runge-Kutta method to solve differential equations, to simulate the inflaton-Higgs coupled system of our interest. We start the calculation from the end of the inflation, i.e., $t = t_*$ (see eq. (2.14)). We take the initial box size $L = 20/\mu$ with the number of grids $N = 128$ per edge. The time step is taken to be $dt = 10^{-3}/\mu$. The scale factor is normalized as $a(t_*) = 1$. We are paying particular attention to the Higgs production by the parametric resonance. Then, we are interested in the Higgs fluctuations with the wave number of the order of $\sim \mu$, corresponding to the wavelength of $\sim \frac{2\pi}{\mu}$. On the contrary, the lattice spacing is $\sim 0.2a(t)\mu^{-1}$ with our choice of the lattice parameters. Then, the lattice spacing may become too large to resolve the Higgs fluctuation from the parametric resonance when $a(t) \gtrsim 10$ or so, which is the case when $\mu t \gtrsim O(10)$. (We found that the scale factor is 5.0, 5.7, and 6.4 for $t = 20\mu^{-1}$, $25\mu^{-1}$, and $30\mu^{-1}$, respectively.) We expect that our numerical calculation is reliable as far as $\mu t \lesssim O(10)$.

For the initial field values of the inflaton and canonically normalized Higgs, we presume that they originate from the quantum fluctuations at $t = t_*$; we firstly evaluate them with neglecting the cosmic expansion. In the lattice simulation, we study the evolutions of the field values at lattice sites $\vec{x} = \frac{L}{N}(n_x, n_y, n_z)$ with $0 \le n_{x,y,z} < N$. The field operators at the lattice sites can be expressed as

$$\hat{X}^{(\text{lattice})}(\vec{x}, t) = \frac{1}{L^{3/2}} \sum_{\vec{k}} \frac{1}{\sqrt{2\omega_k}} \left[\hat{a}_{\vec{k}}(t) e^{i\vec{k}\vec{x}} + \text{h.c.} \right], \tag{4.7}$$

where $X = \phi$ and h_c (see eq. (2.25)). Here, $\vec{k} = \frac{2\pi}{L}(n'_x, n'_y, n'_z)$ with $0 \le n'_{x,y,z} < N$ and $\omega_k^2 = \vec{k}^2 + \partial^2 \tilde{V}/\partial X^2$. Then, after the conventional canonical quantization, we find $[\hat{a}_{\vec{k}}, \hat{a}^\dagger_{\vec{k}'}] = \delta_{\vec{k},\vec{k}'}$ and $\langle \hat{a}_{\vec{k}} \hat{a}^\dagger_{\vec{k}} \rangle = 1$ (with $\langle \cdots \rangle$ being the vacuum expectation value). We set the initial values of the scalar amplitudes as

$$X^{(\text{lattice})}(\vec{x}, t_*) = \frac{1}{L^{3/2}} \sum_{\vec{k}} \frac{1}{\sqrt{2\omega_k}} \left(\tilde{X}_{\vec{k}} e^{i\vec{k}\vec{x}} + \text{c.c.} \right), \tag{4.8}$$

where $\tilde{X}_{\vec{k}}$'s are regarded as statistical variables. The statistical properties of $\tilde{X}_{\vec{k}}$'s are determined so that $\langle \hat{X}^{(\text{lattice})}(\vec{x}, t_*) \hat{X}^{(\text{lattice})}(\vec{x}', t_*) \rangle = \langle X^{(\text{lattice})}(\vec{x}, t_*) X^{(\text{lattice})}(\vec{x}', t_*) \rangle_{\text{stat}}$ (with $\langle \cdots \rangle_{\text{stat}}$ being statistical average). Then, we find $\langle \tilde{X}^*_{\vec{k}} \tilde{X}_{\vec{k}} \rangle_{\text{stat}} = \frac{1}{2}$; in the lattice simulation, $\tilde{X}_{\vec{k}}$'s are sampled by assuming that $\text{Re}\tilde{X}_{\vec{k}}$ and $\text{Im}\tilde{X}_{\vec{k}}$ obey Gaussian distribution $N(0, \frac{1}{4})$. The time dependence of $\tilde{X}_{\vec{k}}$ is given by $\tilde{X}_{\vec{k}} \propto a^{-1} e^{-i\omega_k t}$, and the initial time derivative is

$$\dot{\tilde{X}}_{\vec{k}} = (-i\omega_k - H(t_*))\tilde{X}_{\vec{k}}. \tag{4.9}$$

Finally, fluctuations of the canonically normalized Higgs field and its time derivative are rescaled back to those of the original Higgs field and then added to the homogeneous parts.

In order to check the reliability of our numerical analysis, we have performed the analysis with $N = 256$ (as well as $N = 128$) for $\xi = 1.4$ and 1.8 taking central values of the standard-model couplings. For $\xi = 1.4$, we found that the electroweak vacuum is stable until $\mu t \lesssim 30$ for both choices of the number of grids while two results show difference at a

JHEP09(2022)102

later epoch; at $\mu t \gtrsim 30$, there is no sign of the instability for $N = 128$ while, for $N = 256$, the Higgs variance shows a significant increase. In addition, for $N = 256$, we found that the detail of the behavior at $\mu t \gtrsim 30$ is dependent on the initial configuration. As we have mentioned earlier, the lattice spacing becomes of the same order as the wavelength of our interest when $\mu t \sim O(10)$, which may be the cause of the difference. For $\xi = 1.8$, destabilization happens at $\mu t \sim 20$ both for $N = 128$ and 256 and two choices of the number of grids does not show the qualitative difference.[7] Thus, we expect that our numerical calculation with $N = 128$ is reliable for $\mu t \lesssim 30$ while the results for $\mu t \gtrsim 30$ may be affected by numerical artifacts. In the following, we rely on the numerical results for $\mu t \leq 25$ with taking $N = 128$ to derive a bound on ξ; we could not increase N because of the limitation of the computational resource.

If the destabilization happens, the Higgs variance starts to blow up. The destabilization process may be affected by the scattering (and thermalization) processes of the Higgs field. At the epoch of our interest, i.e., $\mu t \lesssim 30$, we presume that the effects of the scatterings are not important. During such an epoch, the Higgs occupation number η exponentially increases, while the scattering cross section is $\sigma \sim \frac{g^4}{4\pi}\frac{1}{\mu^2}$ (with g being the gauge coupling constant).[8] Then, the scattering rate is $\Gamma_{\rm scatt} \sim \eta\mu^3\sigma \sim \frac{g^4}{4\pi}\eta\mu$. Because the resonance parameter q is at most ~ 1 for the case we consider (see eq. (3.6)) and the redshift effect takes the enhanced modes away from the resonance band, η is not expected to be extremely large and the scattering rate is expected to be smaller than the expansion rate, which is $O(0.1)\mu$ for $\mu t \lesssim 30$. Thus, we neglect the effects of the scattering processes.

In the following, we derive a conservative bound on ξ concentrating on the resonance regime. The time of the end of the resonance regime, denoted as $t_{\rm end}$, is estimated by studying the Higgs dynamics with $\lambda = 0$; the Higgs variance for $\lambda = 0$ is denoted as $\langle h^2\rangle_0$. After $t_{\rm end}$, the peak value of $\langle h^2\rangle_0$ is expected to decrease because the effect of the Hubble friction wins over the effect of the parametric resonance. In figure 3, we show the evolution of $\langle h^2\rangle_0$, taking $\xi = 1.4$ and $\xi = 2.5$. We can see that $\langle h^2\rangle_0$ reaches the highest peak in the time interval of $20 \lesssim \mu t \lesssim 30$; we have checked that, when $1.4 \leq \xi \leq 2.5$, the highest peak is realized during this period. For larger ξ, the parametric resonance stops at a later epoch. In the following, we consider the cases with $1.4 \leq \xi \leq 2.5$ and take $\mu t_{\rm end} = 20$ and 25.

In order to quantify the instability of the electroweak vacuum, we use the fact that the Higgs variance $\langle h^2\rangle$ becomes significantly larger than $\langle h^2\rangle_0$ once the instability occurs. In figure 4, we show the evolutions of $\langle h^2\rangle$ and $\langle h^2\rangle_0$ for $\xi = 1.4$ and 1.8; here we take $c = 20$, 200, and 2000. For the case of $\xi = 1.4$, the instability does not occur and $\langle h^2\rangle$ behaves

[7] We note that N cannot be taken too large because, in the present prescription, the dispersion relation of the Higgs may be significantly altered by the initial fluctuation. Rigorously speaking, a renormalization is necessary to subtract such a correction (cf., ref. [30]). In the present case, however, it is neglected because the effect is unimportant for the study of the parametric resonance. Substituting the initial fluctuation into $\lambda\langle h^2\rangle$, the correction to the Higgs mass squared is estimated to be $\sim \frac{\lambda}{16\pi^2}\frac{(2\pi)^2N^2}{L^2}$. It is smaller than the typical momentum squared relevant for the parametric resonance (i.e., μ^2) as far as $N \lesssim 400\sqrt{\frac{0.01}{|\lambda|}}$. In our calculation, this condition is met.

[8] We do not consider the possibly fast decay process, e.g., $H \to t\bar{t}$, which may be kinematically blocked due to the plasma mass induced by the large Higgs occupation number.

JHEP09(2022)102

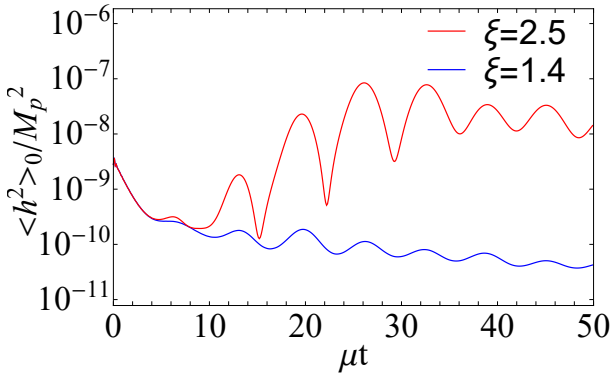

Figure 3. Time evolution of the Higgs field variance $\langle h^2\rangle_0$ for $\lambda = 0$. The non-minimal Higgs-gravity couplings are taken to be $\xi = 1.4$ (blue) and $\xi = 2.5$ (red). We take $\mu t_{\rm end} = 20$ and 25 to derive the upper bound on ξ.

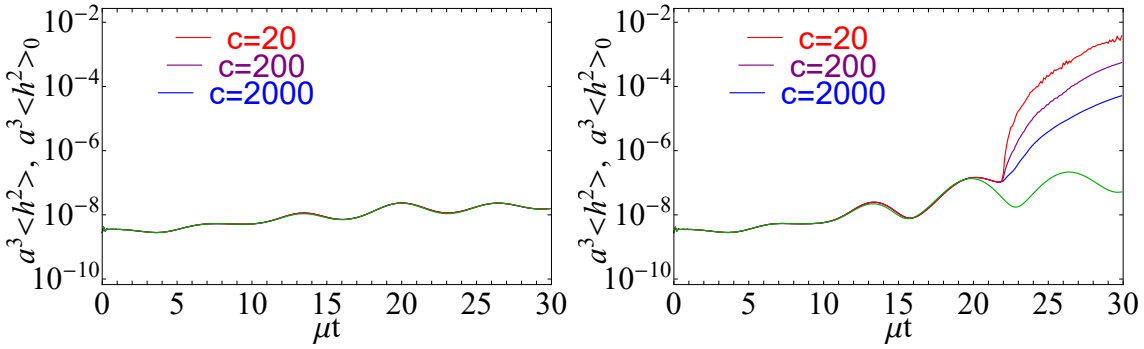

(a) $\xi = 1.4$ (b) $\xi = 1.8$

Figure 4. Lattice simulation results of the Higgs field variance $\langle h^2\rangle$ for $\xi = 1.4$ and 1.8 and varying values of c: 20 (red), 200 (purple) and 2000 (blue). The top quark mass is taken to be $M_t = 172\,\text{GeV}$, and the strong coupling is the central value $\alpha_s = 0.1179$. Time evolution of $\langle h^2\rangle_0$ is shown in green line. Both $\langle h^2\rangle$ and $\langle h^2\rangle_0$ are multiplied by a^3 and normalized by $M_{\rm Pl}^2$.

as $\langle h^2\rangle_0$. With larger value of ξ, $\langle h^2\rangle$ starts to deviate from $\langle h^2\rangle_0$ at $t \sim t_{\rm inst}$ and shows significant increase after $t \sim t_c$; for the case of $\xi = 1.8$ shown in figure 4, $t_{\rm inst} \simeq 20\mu^{-1}$ and $t_c \simeq 22\mu^{-1}$. The Higgs variance at $t \lesssim t_c$ is insensitive to the choice of c. On the contrary, $\langle h^2\rangle$ at $t \gtrsim t_c$ depends on c; we can see that, in such an epoch, $\langle h^2\rangle$ is approximately proportional to $c^{-1}(t - t_c)^3$. We comment that such behavior arises when the universe is filled with the "false vacuum region" with $h \ll h_{\rm min}$ and the "true vacuum bubble," in which $h \sim h_{\rm min}$, whose wall velocity is close to the speed of light.[9] The deviation of $\langle h^2\rangle$

[9]We comment that the observation here indicates a new possibility to realize a relativistic expansion of bubble walls. Let us consider a scalar field s, with its mass smaller than $H_{\rm inf}$, whose potential has a negative quartic coupling and a positive Planck-suppressed higher dimensional term. If s has a non-minimal coupling $\sim s^2R$, s is trapped at the origin during the inflation, and its amplitude may be parametrically enhanced after inflation. The dynamics of s is similar to that of the Higgs studied in our analysis. If the amplification of the amplitude of s is large enough, the tachyonic instability of s may happen, resulting in the formation of bubbles in which s is at the minimum of its potential. The latent energy carried by s once become the

JHEP09(2022)102

from $\langle h^2 \rangle_0$ is expected to be a sign of the instability. In our analysis, we adopt the following criterion for the instability:

$$\left. \frac{\langle h^2 \rangle - \langle h^2 \rangle_0}{\langle h^2 \rangle_0} \right|_{t=t_{\rm end}} > 2. \tag{4.10}$$

With too large ξ, the above condition is met, indicating that the tachyonic mass induced by Higgs self coupling dominates the total effective mass and that the instability of the electroweak vacuum is triggered.

We have studied the behavior of the Higgs variable for several choices of the non-minimal coupling ξ and the top quark mass M_t. We take the non-minimal coupling ξ with the interval of 0.1 and top quark mass in the range of $171.5 - 173.5\,\text{GeV}$ with the interval of $0.5\,\text{GeV}$. The sample points on which we perform the lattice simulation are indicated by the dots on figure 5; for the figure, the central value of the strong coupling constant is used while $\mu t_{\rm end}$ is taken to be 20 and 25. The red dots on the figure show the sample points on which the destabilization is observed (see eq. (4.10)) while the blue ones are sample points without the sign of instability. We have connected the red dots at the boundary, which we regard as an upper bound on the non-minimal coupling. We can see that the upper bound on ξ becomes smaller as the top quark becomes heavier. This is due to the fact that, with larger top quark mass, λ becomes smaller meaning that the absolute value of the tachyonic mass induced by Higgs self coupling is more enhanced (see figure 1).

In order to see how the bound depends on the strong coupling constant, we also perform the lattice simulation for several values of α_s; the result is shown in figure 6 (for which the top quark mass is taken to be the central value $M_t = 172.76$ GeV). As in the case of figure 5, the red and blue dots indicate the sample points with and without the sign of the destabilization before $t_{\rm end}$. We can see that the upper bound becomes larger for larger value of α_s, which is due to the fact that $\lambda(Q)$ with fixed $Q > M_t$ increases with the increase of α_s.

The upper bound on the non-minimal coupling depends slightly on the choice of $t_{\rm end}$. For $20 < \mu t_{\rm end} < 25$, the upper bound varies $\sim O(10)$ % and is larger for smaller $t_{\rm end}$. Adopting the central values of M_t and α_s, the upper bound on ξ is $1.6 - 1.7$. The bound is significantly smaller than the one obtained in the case of conventional inflation models without the R^2 term, which gives $\xi \lesssim 5$ [30, 36].

5 Conclusions and discussion

We have discussed the stability of the electroweak vacuum during and after the Starobinsky inflation. We paid particular attention to the non-minimal coupling of the Higgs to gravity,

kinetic energy of the wall, then transferred to the energy of radiation, e.g., with bubble collisions. Contrary to the case of the standard-model Higgs, a viable cosmological scenario is possible because we may live in a vacuum with a very large amplitude of s. Since the phenomena may be similar to that in the strong first-order phase transition with relativistic bubble expansion, relevant particle production mechanisms may be applicable [61–66]. However, the gravitational waves due to the bubble wall collisions or sound waves may be too high-frequency to be observed in the near future if the inflation scale is high.

JHEP09(2022)102

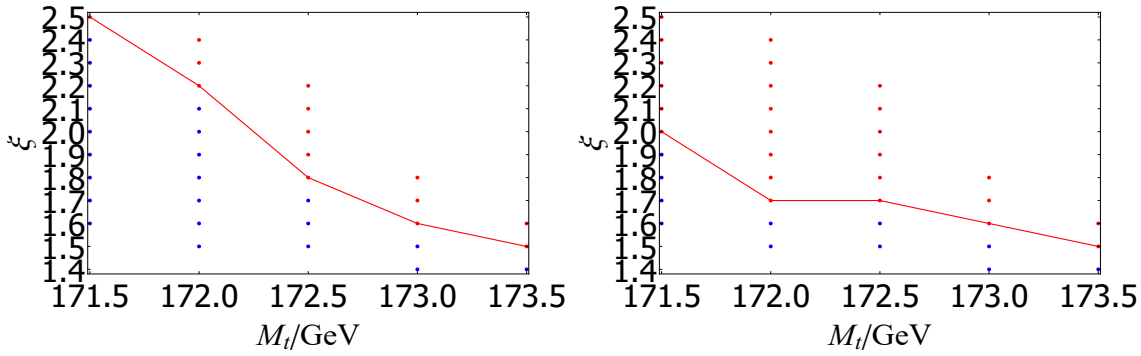

(a) $\mu t_{\rm end} = 20$ (b) $\mu t_{\rm end} = 25$

Figure 5. Vacuum stability bounds on ξ for different values of the top quark mass M_t, taking $\alpha_s = 0.1179$ and $\mu t_{\rm end} = 20$ and 25. The red (blue) dots show the sample points with (without) the instability of the electroweak vacuum. The red line indicates our upper bounds on ξ.

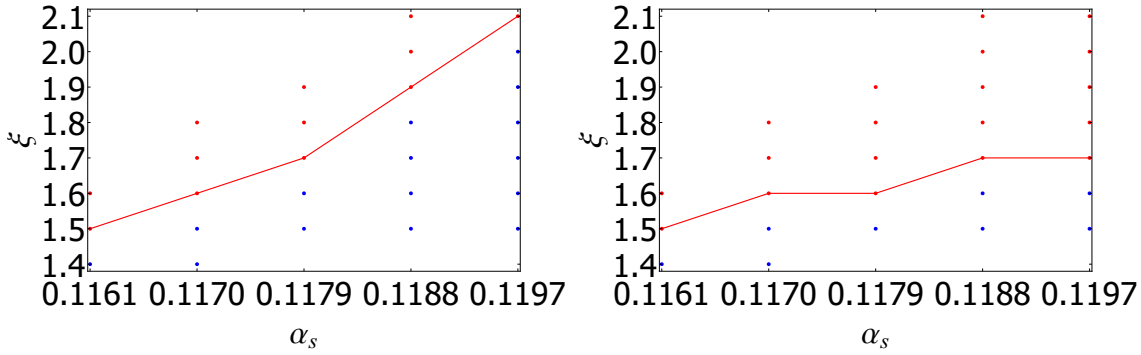

(a) $\mu t_{\rm end} = 20$ (b) $\mu t_{\rm end} = 25$

Figure 6. Vacuum stability bounds on ξ for different values of the strong coupling α_s, taking $M_t = 172.76$ GeV and $\mu t_{\rm end} = 20$ and 25. The red (blue) dots show the sample points with (without) the instability of the electroweak vacuum. The red line indicates our upper bounds on ξ.

and studied the enhancement of the Higgs amplitude due to the parametric resonance after the inflation. Because the Starobinsky inflation requires the expansion rate during inflation to be larger than the instability scale of the Higgs potential in the standard model, the quantum fluctuation during inflation may make the Higgs amplitude larger than the instability scale, resulting in the run-away behavior of the Higgs field. The non-minimal coupling of the Higgs field to the Ricci scalar is introduced to avoid such instability. The non-minimal coupling, however, may induce a parametric-resonance production of the Higgs after inflation, which may destabilize the Higgs amplitude. The effect of the parametric resonance is more enhanced as the non-minimal coupling constant ξ becomes larger.

We have studied the dynamics of the Higgs field in the preheating epoch after inflation in detail in the Starobinsky inflation model. In the case of the Starobinsky inflation, the evolution equation of the Higgs field differs from that in the case of simple inflation

JHEP09(2022)102

models (which are based on the Einstein-Hilbert action without the R^2 term). We used the numerical lattice simulation to follow the evolution of the Higgs field and investigated the stability of the Higgs amplitude. We have seen that the Higgs amplitude is destabilized if the non-minimal coupling constant ξ is large. With requiring that the Higgs amplitude does not show the run-away behavior, we derived an upper bound on the non-minimal coupling constant ξ. With the central values of the standard-model parameters, for example, we found that ξ should be smaller than $\sim 1.6 - 1.7$ in order to realize the electroweak vacuum in the present universe.

Acknowledgments

This work was supported by JSPS KAKENHI Grant Numbers 16H06490 [TM], 22H01215 [TM, WY], 17H06359 [KN], 18K03609 [KN], 20H05851 [WY], 21K20364 [WY] and 22K14029 [WY].

References

[1] M. Sher, *Electroweak Higgs Potentials and Vacuum Stability*, *Phys. Rept.* **179** (1989) 273 [INSPIRE].

[2] P.B. Arnold, *Can the Electroweak Vacuum Be Unstable?*, *Phys. Rev. D* **40** (1989) 613 [INSPIRE].

[3] G.W. Anderson, *New Cosmological Constraints on the Higgs Boson and Top Quark Masses*, *Phys. Lett. B* **243** (1990) 265 [INSPIRE].

[4] P.B. Arnold and S. Vokos, *Instability of hot electroweak theory: bounds on m(H) and M(t)*, *Phys. Rev. D* **44** (1991) 3620 [INSPIRE].

[5] J.R. Espinosa and M. Quirós, *Improved metastability bounds on the standard model Higgs mass*, *Phys. Lett. B* **353** (1995) 257 [hep-ph/9504241] [INSPIRE].

[6] G. Isidori, G. Ridolfi and A. Strumia, *On the metastability of the standard model vacuum*, *Nucl. Phys. B* **609** (2001) 387 [hep-ph/0104016] [INSPIRE].

[7] J.R. Espinosa, G.F. Giudice and A. Riotto, *Cosmological implications of the Higgs mass measurement*, *JCAP* **05** (2008) 002 [arXiv:0710.2484] [INSPIRE].

[8] J. Ellis, J.R. Espinosa, G.F. Giudice, A. Hoecker and A. Riotto, *The Probable Fate of the Standard Model*, *Phys. Lett. B* **679** (2009) 369 [arXiv:0906.0954] [INSPIRE].

[9] J. Elias-Miro, J.R. Espinosa, G.F. Giudice, G. Isidori, A. Riotto and A. Strumia, *Higgs mass implications on the stability of the electroweak vacuum*, *Phys. Lett. B* **709** (2012) 222 [arXiv:1112.3022] [INSPIRE].

[10] F. Bezrukov, M.Y. Kalmykov, B.A. Kniehl and M. Shaposhnikov, *Higgs Boson Mass and New Physics*, *JHEP* **10** (2012) 140 [arXiv:1205.2893] [INSPIRE].

JHEP09(2022)102

[11] G. Degrassi et al., *Higgs mass and vacuum stability in the Standard Model at NNLO*, *JHEP* **08** (2012) 098 [arXiv:1205.6497] [INSPIRE].

[12] D. Buttazzo et al., *Investigating the near-criticality of the Higgs boson*, *JHEP* **12** (2013) 089 [arXiv:1307.3536] [INSPIRE].

[13] A.V. Bednyakov, B.A. Kniehl, A.F. Pikelner and O.L. Veretin, *Stability of the Electroweak Vacuum: Gauge Independence and Advanced Precision*, *Phys. Rev. Lett.* **115** (2015) 201802 [arXiv:1507.08833] [INSPIRE].

[14] A. Salvio, A. Strumia, N. Tetradis and A. Urbano, *On gravitational and thermal corrections to vacuum decay*, *JHEP* **09** (2016) 054 [arXiv:1608.02555] [INSPIRE].

[15] A. Andreassen, W. Frost and M.D. Schwartz, *Scale Invariant Instantons and the Complete Lifetime of the Standard Model*, *Phys. Rev. D* **97** (2018) 056006 [arXiv:1707.08124] [INSPIRE].

[16] S. Chigusa, T. Moroi and Y. Shoji, *State-of-the-Art Calculation of the Decay Rate of Electroweak Vacuum in the Standard Model*, *Phys. Rev. Lett.* **119** (2017) 211801 [arXiv:1707.09301] [INSPIRE].

[17] S. Chigusa, T. Moroi and Y. Shoji, *Decay Rate of Electroweak Vacuum in the Standard Model and Beyond*, *Phys. Rev. D* **97** (2018) 116012 [arXiv:1803.03902] [INSPIRE].

[18] A. Kobakhidze and A. Spencer-Smith, *Electroweak Vacuum (In)Stability in an Inflationary Universe*, *Phys. Lett. B* **722** (2013) 130 [arXiv:1301.2846] [INSPIRE].

[19] M. Fairbairn and R. Hogan, *Electroweak Vacuum Stability in light of BICEP2*, *Phys. Rev. Lett.* **112** (2014) 201801 [arXiv:1403.6786] [INSPIRE].

[20] A. Hook, J. Kearney, B. Shakya and K.M. Zurek, *Probable or Improbable Universe? Correlating Electroweak Vacuum Instability with the Scale of Inflation*, *JHEP* **01** (2015) 061 [arXiv:1404.5953] [INSPIRE].

[21] M. Herranen, T. Markkanen, S. Nurmi and A. Rajantie, *Spacetime curvature and the Higgs stability during inflation*, *Phys. Rev. Lett.* **113** (2014) 211102 [arXiv:1407.3141] [INSPIRE].

[22] K. Kamada, *Inflationary cosmology and the standard model Higgs with a small Hubble induced mass*, *Phys. Lett. B* **742** (2015) 126 [arXiv:1409.5078] [INSPIRE].

[23] J. Kearney, H. Yoo and K.M. Zurek, *Is a Higgs Vacuum Instability Fatal for High-Scale Inflation?*, *Phys. Rev. D* **91** (2015) 123537 [arXiv:1503.05193] [INSPIRE].

[24] J.R. Espinosa et al., *The cosmological Higgstory of the vacuum instability*, *JHEP* **09** (2015) 174 [arXiv:1505.04825] [INSPIRE].

[25] A. Joti et al., *(Higgs) vacuum decay during inflation*, *JHEP* **07** (2017) 058 [arXiv:1706.00792] [INSPIRE].

[26] G. Franciolini, G.F. Giudice, D. Racco and A. Riotto, *Implications of the detection of primordial gravitational waves for the Standard Model*, *JCAP* **05** (2019) 022 [arXiv:1811.08118] [INSPIRE].

[27] A. Mantziris, T. Markkanen and A. Rajantie, *Vacuum decay constraints on the Higgs curvature coupling from inflation*, *JCAP* **03** (2021) 077 [arXiv:2011.03763] [INSPIRE].

[28] V. De Luca, A. Kehagias and A. Riotto, *On the Cosmological Stability of the Higgs Instability*, arXiv:2205.10240 [INSPIRE].

JHEP09(2022)102

[29] M. Herranen, T. Markkanen, S. Nurmi and A. Rajantie, *Spacetime curvature and Higgs stability after inflation*, *Phys. Rev. Lett.* **115** (2015) 241301 [arXiv:1506.04065] [INSPIRE].

[30] Y. Ema, K. Mukaida and K. Nakayama, *Fate of Electroweak Vacuum during Preheating*, *JCAP* **10** (2016) 043 [arXiv:1602.00483] [INSPIRE].

[31] K. Kohri and H. Matsui, *Higgs vacuum metastability in primordial inflation, preheating, and reheating*, *Phys. Rev. D* **94** (2016) 103509 [arXiv:1602.02100] [INSPIRE].

[32] K. Enqvist, M. Karciauskas, O. Lebedev, S. Rusak and M. Zatta, *Postinflationary vacuum instability and Higgs-inflaton couplings*, *JCAP* **11** (2016) 025 [arXiv:1608.08848] [INSPIRE].

[33] M. Postma and J. van de Vis, *Electroweak stability and non-minimal coupling*, *JCAP* **05** (2017) 004 [arXiv:1702.07636] [INSPIRE].

[34] Y. Ema, M. Karciauskas, O. Lebedev and M. Zatta, *Early Universe Higgs dynamics in the presence of the Higgs-inflaton and non-minimal Higgs-gravity couplings*, *JCAP* **06** (2017) 054 [arXiv:1703.04681] [INSPIRE].

[35] Y. Ema, K. Mukaida and K. Nakayama, *Electroweak Vacuum Metastability and Low-scale Inflation*, *JCAP* **12** (2017) 030 [arXiv:1706.08920] [INSPIRE].

[36] D.G. Figueroa, A. Rajantie and F. Torrenti, *Higgs field-curvature coupling and postinflationary vacuum instability*, *Phys. Rev. D* **98** (2018) 023532 [arXiv:1709.00398] [INSPIRE].

[37] S. Rusak, *Destabilization of the EW vacuum in non-minimally coupled inflation*, *JCAP* **05** (2020) 020 [arXiv:1811.10569] [INSPIRE].

[38] J. Kost, C.S. Shin and T. Terada, *Massless preheating and electroweak vacuum metastability*, *Phys. Rev. D* **105** (2022) 043508 [arXiv:2105.06939] [INSPIRE].

[39] A.D. Dolgov and D.P. Kirilova, *On particle creation by a time dependent scalar field*, *Sov. J. Nucl. Phys.* **51** (1990) 172 [INSPIRE].

[40] J.H. Traschen and R.H. Brandenberger, *Particle Production During Out-of-equilibrium Phase Transitions*, *Phys. Rev. D* **42** (1990) 2491 [INSPIRE].

[41] L. Kofman, A.D. Linde and A.A. Starobinsky, *Reheating after inflation*, *Phys. Rev. Lett.* **73** (1994) 3195 [hep-th/9405187] [INSPIRE].

[42] Y. Shtanov, J.H. Traschen and R.H. Brandenberger, *Universe reheating after inflation*, *Phys. Rev. D* **51** (1995) 5438 [hep-ph/9407247] [INSPIRE].

[43] L. Kofman, A.D. Linde and A.A. Starobinsky, *Towards the theory of reheating after inflation*, *Phys. Rev. D* **56** (1997) 3258 [hep-ph/9704452] [INSPIRE].

[44] B.A. Bassett and S. Liberati, *Geometric reheating after inflation*, *Phys. Rev. D* **58** (1998) 021302 [*Erratum ibid.* **60** (1999) 049902] [hep-ph/9709417] [INSPIRE].

[45] S. Tsujikawa, K.-i. Maeda and T. Torii, *Resonant particle production with nonminimally coupled scalar fields in preheating after inflation*, *Phys. Rev. D* **60** (1999) 063515 [hep-ph/9901306] [INSPIRE].

[46] J.F. Dufaux, G.N. Felder, L. Kofman, M. Peloso and D. Podolsky, *Preheating with trilinear interactions: Tachyonic resonance*, *JCAP* **07** (2006) 006 [hep-ph/0602144] [INSPIRE].

[47] A.A. Starobinsky, *A New Type of Isotropic Cosmological Models Without Singularity*, *Phys. Lett. B* **91** (1980) 99 [INSPIRE].

JHEP09(2022)102

[48] Planck collaboration, *Planck 2018 results. X. Constraints on inflation*, *Astron. Astrophys.* **641** (2020) A10 [arXiv:1807.06211] [INSPIRE].

[49] D.S. Gorbunov and A.G. Panin, *Scalaron the mighty: producing dark matter and baryon asymmetry at reheating*, *Phys. Lett. B* **700** (2011) 157 [arXiv:1009.2448] [INSPIRE].

[50] D.S. Gorbunov and A.G. Panin, *Free scalar dark matter candidates in R^2-inflation: the light, the heavy and the superheavy*, *Phys. Lett. B* **718** (2012) 15 [arXiv:1201.3539] [INSPIRE].

[51] N. Bernal, J. Rubio and H. Veermäe, *UV Freeze-in in Starobinsky Inflation*, *JCAP* **10** (2020) 021 [arXiv:2006.02442] [INSPIRE].

[52] Q. Li, T. Moroi, K. Nakayama and W. Yin, *Hidden dark matter from Starobinsky inflation*, *JHEP* **09** (2021) 179 [arXiv:2105.13358] [INSPIRE].

[53] K.-i. Maeda, *Towards the Einstein-Hilbert Action via Conformal Transformation*, *Phys. Rev. D* **39** (1989) 3159 [INSPIRE].

[54] Planck collaboration, *Planck 2018 results. VI. Cosmological parameters*, *Astron. Astrophys.* **641** (2020) A6 [*Erratum ibid.* **652** (2021) C4] [arXiv:1807.06209] [INSPIRE].

[55] BICEP and Keck collaborations, *Improved Constraints on Primordial Gravitational Waves using Planck, WMAP, and BICEP/Keck Observations through the 2018 Observing Season*, *Phys. Rev. Lett.* **127** (2021) 151301 [arXiv:2110.00483] [INSPIRE].

[56] Particle Data Group collaboration, *Review of Particle Physics*, *PTEP* **2020** (2020) 083C01 [INSPIRE].

[57] S.P. Martin and D.G. Robertson, *Standard model parameters in the tadpole-free pure $\overline{\text{MS}}$ scheme*, *Phys. Rev. D* **100** (2019) 073004 [arXiv:1907.02500] [INSPIRE].

[58] T. Moroi and W. Yin, *Light Dark Matter from Inflaton Decay*, *JHEP* **03** (2021) 301 [arXiv:2011.09475] [INSPIRE].

[59] T. Moroi and W. Yin, *Particle Production from Oscillating Scalar Field and Consistency of Boltzmann Equation*, *JHEP* **03** (2021) 296 [arXiv:2011.12285] [INSPIRE].

[60] H.L. Child, J.T. Giblin Jr, R.H. Ribeiro and D. Seery, *Preheating with Non-Minimal Kinetic Terms*, *Phys. Rev. Lett.* **111** (2013) 051301 [arXiv:1305.0561] [INSPIRE].

[61] A. Falkowski and J.M. No, *Non-thermal Dark Matter Production from the Electroweak Phase Transition: Multi-TeV WIMPs and 'Baby-Zillas'*, *JHEP* **02** (2013) 034 [arXiv:1211.5615] [INSPIRE].

[62] A. Katz and A. Riotto, *Baryogenesis and Gravitational Waves from Runaway Bubble Collisions*, *JCAP* **11** (2016) 011 [arXiv:1608.00583] [INSPIRE].

[63] A. Azatov and M. Vanvlasselaer, *Bubble wall velocity: heavy physics effects*, *JCAP* **01** (2021) 058 [arXiv:2010.02590] [INSPIRE].

[64] A. Azatov, M. Vanvlasselaer and W. Yin, *Dark Matter production from relativistic bubble walls*, *JHEP* **03** (2021) 288 [arXiv:2101.05721] [INSPIRE].

[65] A. Azatov, M. Vanvlasselaer and W. Yin, *Baryogenesis via relativistic bubble walls*, *JHEP* **10** (2021) 043 [arXiv:2106.14913] [INSPIRE].

[66] I. Baldes, S. Blasi, A. Mariotti, A. Sevrin and K. Turbang, *Baryogenesis via relativistic bubble expansion*, *Phys. Rev. D* **104** (2021) 115029 [arXiv:2106.15602] [INSPIRE].

JHEP09(2022)102